Linking electrical and thermal conductivity through cross-property inclusion modelling

Materials Letters: X 12 (2021) 100101

Contents lists available at ScienceDirect

Materials Letters: X

journal homepage: www.sciencedirect.com/journal/materials-letters-x

Linking electrical and thermal conductivity through cross-property inclusion modelling

Phillip A. Cilli [a,*], Mark Chapman [b]

[a] Department of Earth Sciences, University of Oxford, South Parks Road, Oxford OX1 3AN, UK
[b] School of Geosciences, University of Edinburgh, James Hutton Rd, The King's Buildings, Edinburgh EH9 3FE, UK

ARTICLE INFO

Keywords:
Cross-property modelling
Thermal conductivity
Electrical conductivity
DEM
Inclusion modelling

ABSTRACT

We derive a new cross-property differential effective medium scheme for a composite material's thermal conductivity as a function of its electrical conductivity and vice versa. Our scheme assumes that one phase is embedded in the other as inclusions. The relations are independent of inclusion volume fraction, but depend on the aspect ratio of the inclusions. We show that the method successfully models published laboratory measurements on a copper-graphite composite, with the inferred aspect ratio matching the physical shape of the inclusions. This work complements earlier results on elastic-electrical cross-property differential effective medium modelling, and has the potential to be extended for different cross-property relationships.

1. Introduction

The relations linking a composite's effective physical properties, known as cross-property relations, can be useful when one of the composite's properties is easier to measure than that which we wish to quantify [1]. Rigorous cross-property bounds (e.g., [2,1,3]) and exact relations (e.g., [4–6]) have been developed to this end.

More recently, Cilli and Chapman [7] derived a simple cross-property model from first principles with a single model parameter and no phase volume fraction terms. Their model - a differential effective medium (DEM) approximation (e.g., [8,9]) - accurately estimated the elastic properties of brine-saturated clean sandstone cores from electrical conductivity measurements, and vice versa.

Here we extend this cross-property DEM approximation to model the relationship between a composite's thermal and electrical conductivities. We find the model accurately fits the thermal-electrical measurements of Mazloum et al. [10] made on copper-graphite composites and that there is good agreement between the best-fitting model parameter, inclusion aspect ratio, and the experimentally measured aspect ratio of the graphite flake inclusions.

2. Theory

2.1. Electrical and thermal modelling

The electrical DEM approximation for a two-phase composite containing ellipsoidal inclusions can be expressed as [11]

$$\frac{d\boldsymbol{\sigma}_e}{d\phi} = \frac{(\boldsymbol{\sigma}_2 - \boldsymbol{\sigma}_e)\boldsymbol{R}^{(2e)}}{(1-\phi)}, \tag{1}$$

where $\boldsymbol{\sigma}_e$ is the effective electrical conductivity tensor, $\boldsymbol{\sigma}_2$ is the conductivity tensor of the inclusion phase, ϕ is the inclusion volume fraction, and

$$\boldsymbol{R}^{(2e)} = \left[\boldsymbol{I} + \boldsymbol{A}^* \cdot \boldsymbol{\sigma}_e^{-1} \cdot (\boldsymbol{\sigma}_2 - \boldsymbol{\sigma}_e)\right]^{-1}, \tag{2}$$

where $\boldsymbol{A}^*$, a function of inclusion aspect ratio α, is the depolarisation tensor for an ellipsoid in a matrix with an effective conductivity tensor $\boldsymbol{\sigma}_e$ [11]. Eq. 1 is solved with boundary condition $\boldsymbol{\sigma}_e(\phi = 0) = \boldsymbol{\sigma}_1$, where $\boldsymbol{\sigma}_1$ is the background material's electrical conductivity tensor.

In the case of randomly oriented spheroidal inclusions in an isotropic background material, the isotropic form of Eq. 1 approximates the medium's effective isotropic properties regardless of the inclusion phase's intrinsic anisotropy. This isotropic DEM approximation is [11]

* Corresponding author.
E-mail address: Phillip.Cilli@earth.ox.ac.uk (P.A. Cilli).

https://doi.org/10.1016/j.mlblux.2021.100101

Available online 20 September 2021

$$\frac{d\sigma_e}{d\phi} = \frac{(\sigma_2 - \sigma_e)R^{(2e)}}{(1-\phi)}, \tag{3}$$

where σ_e is the isotropic effective conductivity, σ_2 is the isotropic effective conductivity of randomly oriented inclusions, and $R^{(2e)} = \mathrm{Tr}(\boldsymbol{R}^{(2e)})/3$, which evaluates to

$$R^{(2e)} = \frac{1}{3}\sigma_e\left[\frac{4}{\sigma_e + \sigma_2 + L(\sigma_e - \sigma_2)} + \frac{1}{\sigma_e - L(\sigma_e - \sigma_2)}\right], \tag{4}$$

with principal depolarisation factor L (e.g., [12]). Eq. 3 is solved with boundary condition $\sigma_e(\phi = 0) = \sigma_1$, where σ_1 is the background material's isotropic electrical conductivity.

Here, we model a material with randomly oriented anisotropic spheroidal inclusions embedded in an isotropic background material, which thereby possesses an isotropic effective electrical conductivity. This composite's thermal conductivity, electrical permittivity, magnetic permeability, and diffusion constant can also be modelled using inclusion models [11,13] such as Eq. 3. Accordingly, we replace electrical conductivity terms σ with thermal conductivity terms κ in Eqs. 3 and 4 to estimate this composite's effective thermal conductivity, obtaining [11]

$$\frac{d\kappa_e}{d\phi} = \frac{(\kappa_2 - \kappa_e)W^{(2e)}}{(1-\phi)}, \tag{5}$$

where

$$W^{(2e)} = \frac{1}{3}\kappa_e\left[\frac{4}{\kappa_e + \kappa_2 + L(\kappa_e - \kappa_2)} + \frac{1}{\kappa_e - L(\kappa_e - \kappa_2)}\right]. \tag{6}$$

Eq. 5 is solved with boundary condition $\kappa_e(\phi = 0) = \kappa_1$, where κ_1 is the background material's thermal conductivity.

2.2. Thermal-electrical modelling

We apply the chain rule to Eqs. 3 and 5 to obtain the thermal-electrical cross-property DEM model

$$\frac{d\kappa_e}{d\sigma_e} = \frac{(\kappa_2 - \kappa_e)}{(\sigma_2 - \sigma_e)}\frac{W^{(2e)}}{R^{(2e)}}. \tag{7}$$

The inverse of Eq. 7 is its reciprocal and a forward model in its own right:

$$\frac{d\sigma_e}{d\kappa_e} = \frac{(\sigma_2 - \sigma_e)}{(\kappa_2 - \kappa_e)}\frac{R^{(2e)}}{W^{(2e)}}. \tag{8}$$

Eq. 7 has boundary condition $\kappa_e(\sigma_e = \sigma_1) = \kappa_1$ and Eq. 8 has boundary condition $\sigma_e(\kappa_e = \kappa_1) = \sigma_1$. Theoretically, the mathematical form of Eqs. 7 and 8 generalises to relate any two of the composite's effective thermal conductivity, electrical conductivity, electrical permittivity, magnetic permeability, and diffusion constant.

In the cases of spherical (S) inclusions ($\alpha = 1, L = 1/3$), disk-shaped (D) inclusions ($\alpha = 0, L = 1$), and needle-shaped (N) inclusions ($\alpha = \infty$, $L = 0$), Eq. 7 simplifies to

$$\left.\frac{d\kappa_e}{d\sigma_e}\right|_S = \frac{\kappa_e}{\sigma_e}\frac{(\kappa_2 - \kappa_e)}{(\sigma_2 - \sigma_e)}\frac{(2\sigma_e + \sigma_2)}{(2\kappa_e + \kappa_2)}; \tag{9}$$

$$\left.\frac{d\kappa_e}{d\sigma_e}\right|_D = \frac{\sigma_2}{\kappa_2}\frac{(\kappa_2 - \kappa_e)}{(\sigma_2 - \sigma_e)}\frac{(2\kappa_2 + \kappa_e)}{(2\sigma_2 + \sigma_e)}; \tag{10}$$

$$\left.\frac{d\kappa_e}{d\sigma_e}\right|_N = \frac{(\sigma_2 + \sigma_e)}{(\kappa_2 + \kappa_e)}\frac{(\kappa_2 - \kappa_e)}{(\sigma_2 - \sigma_e)}\frac{(\kappa_2 + 5\kappa_e)}{(\sigma_2 + 5\sigma_e)}. \tag{11}$$

The analogous special cases of Eq. 8 for spherical, disk-, and needle-shaped inclusions are the reciprocals of Eqs. (9)–(11) respectively.

3. Method

We modelled the thermal-electrical laboratory measurements of Mazloum et al. [10] made on five samples of copper containing randomly oriented graphite flakes with volume fractions of 0, 0.1, 0.3, 0.4, and 0.5, and an experimentally measured aspect ratio of 0.1.

Following Mazloum et al. [10] after Kováčik and Emmer [14] and Kováčik and Bielekt [15], the graphite thermal and electrical conductivities were 274 W/m K and 0.59×10^{-8} 1/Ω m respectively along a flake's short axis, and 10 W/m K and 2.26×10^{-8} 1/Ω m respectively along its long axes. The copper had isotropic thermal and electrical conductivities of 348.6 W/m K and 58.8×10^{-8} 1/Ω m respectively.

To assess the cross-property DEM approximation's performance on these samples, we aimed to invert Eq. 7 for the unknown inclusion aspect ratio then compare this with the laboratory-measured inclusion aspect ratio. However, the effective isotropic electrical and thermal conductivities of the randomly oriented anisotropic inclusions were also unknown. Thus, we inverted Eq. 7 for all three parameters simultaneously by minimising the l_2-norm of the misfits in measured and modelled thermal conductivity, using the samples' known effective and background conductivities as input. We excluded the 50% graphite sample from this inversion as the model assumes a low inclusion concentration.

We then forward modelled effective thermal and electrical conductivity trends using Eqs. 7 and 8 respectively for inclusion aspect ratios $\alpha \in \{0, 10^{-2}, 10^{-1}, 1, \infty\}$ along with the thermal-electrical Hashin–Shtrikman bounds (e.g., [16]).

4. Results and Discussion

The solved effective inclusion thermal and electrical conductivities were 24.1 W/m K and 0.61×10^{-8} 1/Ω m respectively. Interestingly, both effective inclusion conductivities were close to those along the graphite flakes' symmetry axes which respectively possessed lower conductivities. The solved inclusion aspect ratio was 0.097, which shows good agreement with the experimentally measured aspect ratio of 0.1.

Fig. 1 shows forward modelled thermal and electrical conductivity trends produced using Eqs. 7 and 8. The model is asymptotically correct and the $\alpha = 0.1$ trend fits the measurements on samples containing up to 40% graphite. The modelled trend for disk-shaped inclusions seems to fall on the lower Hashin–Shtrikman bound, which may be expected as single-property DEM approximations can equal the lower Hashin–Shtrikman bound in the case of disk-shaped inclusions [17].

The agreement between modelled and measured inclusion aspect ratio occurs as the composites obey the physical assumptions of the model reasonably well. This contrasts with porous rocks, where inclusion modelling assumptions are often violated and modelled aspect ratios do not obviously relate to pore space architectures (e.g., [18,19]).

5. Conclusions

We have derived a cross-property model which relates a composite's thermal and electrical conductivities. This model is independent of inclusion volume fraction, depending only on inclusion shape. We have modelled published data and observed good agreement between the measured and inverted inclusion aspect ratios. This work builds on a similar electrical-elastic model, and we note its potential to extend to other cross-property relations.

CRediT authorship contribution statement

Phillip A. Cilli: Conceptualization, Methodology, Software, Formal analysis, Investigation, Resources, Writing - original draft, Writing - review & editing, Visualization, Project administration. **Mark**

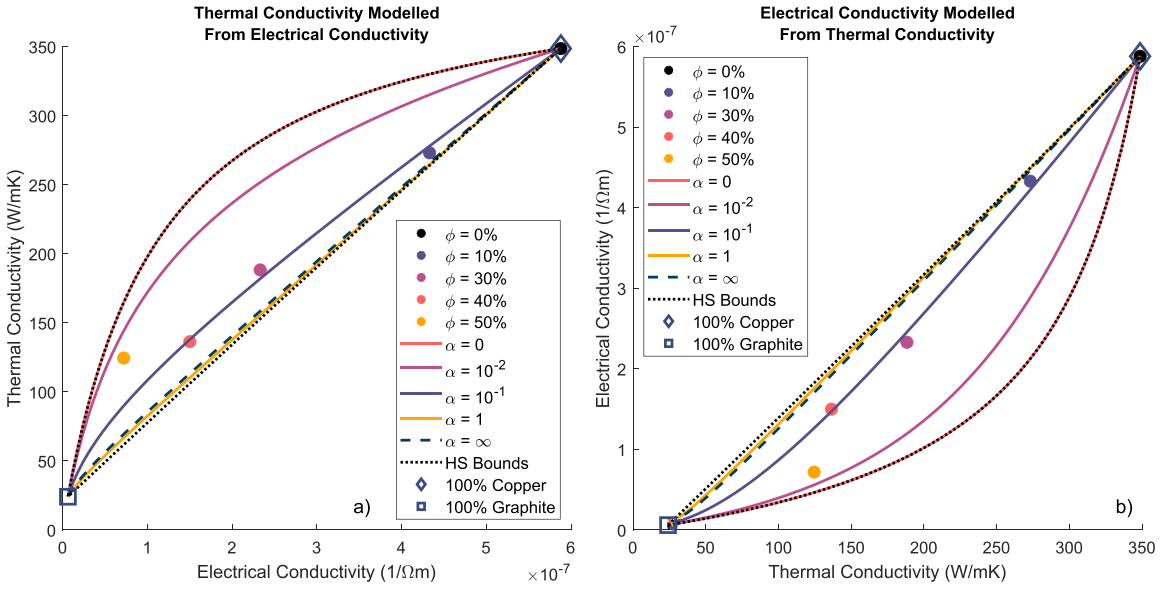

Fig. 1. Thermal-electrical modelling using cross-property DEM. Forward modelled (a) thermal and (b) electrical conductivity trends are generated by solving Eqs. 7 and 8 respectively. No trends are outside the Hashin–Shtrikman (dotted) bounds. All trends converge at the high (square) and low (diamond) inclusion volume fraction limits. Measurements (circles) with graphite content ranging from 0–40% lie near the modelled curve for $\alpha = 0.1$, which is the experimentally measured aspect ratio.

Chapman: Conceptualization, Methodology, Writing - original draft, Writing - review & editing.

Declaration of Competing Interest

The authors declare that they have no known competing financial interests or personal relationships that could have appeared to influence the work reported in this paper.

Acknowledgements

The authors would like to thank Professor Tony Watts at the University of Oxford for his support in this work. This research did not receive any specific grant from funding agencies in the public, commercial, or not-for-profit sectors.

References

[1] L. Gibiansky, S. Torquato, Bounds on the effective moduli of cracked materials, J. Mech. Phys. Solids 44 (1996) 233–242.
[2] G.W. Milton, The Theory of Composites. Cambridge Monographs on Applied and Computational Mathematics, Cambridge University Press, 2002.
[3] G. Mavko, N. Saxena, Embedded-bound method for estimating the change in bulk modulus under either fluid or solid substitution, Geophysics 78 (2013) L87–L99.
[4] V.M. Levin, Thermal expansion coefficient of heterogeneous materials, Mech. Solids 2 (1967) 58–61.
[5] W. Pabst, E. Gregorová, Cross-property relations between elastic and thermal properties of porous ceramics, Adv. Sci. Technol., Trans. Tech. Publ. (2006) 107–112.
[6] I. Sevostianov, M. Kachanov, Explicit cross-property correlations for anisotropic two-phase composite materials, J. Mech. Phys. Solids 50 (2002) 253–282.
[7] P.A. Cilli, M. Chapman, Linking elastic and electrical properties of rocks using cross-property DEM, Geophys. J. Int. 225 (2021) 1812–1823.
[8] J.G. Berryman, Single-scattering approximations for coefficients in Biot's equations of poroelasticity, J. Acoust. Society Am. 91 (1992) 551–571.
[9] K.S. Mendelson, M.H. Cohen, The effect of grain anisotropy on the electrical properties of sedimentary rocks, Geophysics 47 (1982) 257–263.
[10] A. Mazloum, J. Kováčik, Š. Emmer, I. Sevostianov, Copper–graphite composites: Thermal expansion, thermal and electrical conductivities, and cross-property connections, J. Mater. Sci. 51 (2016) 7977–7990.
[11] S. Torquato, Random heterogeneous materials: Microstructure and macroscopic properties, Springer-Verlag, New York, 2002.
[12] J.A. Osborn, Demagnetizing factors of the general ellipsoid, Phys. Rev. 76 (1945) 351–357.
[13] T. Choy, Effective Medium Theory: Principles and Applications. International Series of Monographs on Physics, Oxford University Press, 2016.
[14] J. Kováčik, Š. Emmer, Thermal expansion of Cu/graphite composites: Effect of copper coating, Kovove Mater 49 (2011) 411–416.
[15] J. Kováčik, J. Bielekt, Electrical conductivity of Cu/graphite composite material, as a function of structural characteristics, Scripta materialia 35 (1996) 151–156.
[16] J.M. Carcione, B. Ursin, J.I. Nordskag, Cross-property relations between electrical conductivity and the seismic velocity of rocks, Geophysics 72 (2007) E193–E204.
[17] A.N. Norris, A differential scheme for the effective moduli of composites, Mech. Mater. 4 (1985) 1–16.
[18] P.A. Cilli, M. Chapman, The power-law relation between inclusion aspect ratio and porosity: Implications for electrical and elastic modeling, J. Geophys. Res.: Solid Earth 125 (2020) 1–25.
[19] J. Singh, P.A. Cilli, A. Hosa, I. Main, Digital rock physics in four dimensions: Simulating cementation and its effect on seismic velocity, Geophys. J. Int. 222 (2020) 1606–1619.